PROCEEDINGS OF SCIENCE

Exclusive ρ^0 Meson Photoproduction with a Leading Neutron at HERA

Sergey Levonian[*†]
DESY, Notkestraße 85, 22607 Hamburg, Germany
E-mail: levonian@mail.desy.de

A first measurement is presented of exclusive photoproduction of ρ^0 mesons associated with leading neutrons at HERA. The data were taken with the H1 detector in the years 2006 and 2007 at a centre-of-mass energy of $\sqrt{s} = 319$ GeV and correspond to an integrated luminosity of 1.16 pb^{-1}. The ρ^0 mesons with transverse momenta $p_T < 1$ GeV are reconstructed from their decays to charged pions, while leading neutrons carrying a large fraction of the incoming proton momentum, $x_L > 0.35$, are detected in the Forward Neutron Calorimeter. The phase space of the measurement is defined by the photon virtuality $Q^2 < 2$ GeV^2, the total energy of the photon-proton system $20 < W_{\gamma p} < 100$ GeV and the polar angle of the leading neutron $\theta_n < 0.75$ mrad. The cross section of the reaction $\gamma p \to \rho^0 n \pi^+$ is measured as a function of several variables. The data are interpreted in terms of a double peripheral process, involving pion exchange at the proton vertex followed by elastic photoproduction of a ρ^0 meson on the virtual pion. In the framework of one-pion-exchange dominance the elastic cross section of photon-pion scattering, $\sigma^{\rm el}(\gamma\pi^+ \to \rho^0\pi^+)$, is extracted. The value of this cross section indicates significant absorptive corrections for the exclusive reaction $\gamma p \to \rho^0 n \pi^+$.

XXIV International Workshop on Deep-Inelastic Scattering and Related Subjects
11-15 April, 2016
DESY Hamburg, Germany

[*]Speaker.
[†]On behalf of the H1 Collaboration.

1. Introduction

The aim of the analysis is to measure exclusive ρ^0 production on virtual pion in the photoproduction regime at HERA and to extract for the first time experimentally elastic $\gamma\pi$ cross section. In the Regge framework the events of such class are explained by the diagram shown in Fig. 1a which involves an exchange of two Regge trajectories in the process $2 \to 3$, known as *Double Peripheral Process* (DPP), or Double-Regge-pole exchange reaction [1]. It has been demonstrated in similar reactions at fixed target experiments that two further diagrams (Fig. 1b, 1c) have to be included in addition to the pion exchange (Fig. 1a), as well as interference between them [2]. However at small values of four-momentum transfer squared t the contributions from graphs 1b and 1c largely cancel and the one-pion-exchange (OPE) term dominates the cross section.

Events of this type are modelled by the two-step Monte Carlo generator POMPYT [3] in which the virtual pion is produced at the proton vertex according to one of the available pion flux parametrisations. This pion then scatters elastically on the photon from the electron beam, thus producing vector meson (ρ^0 in our case). Diffractive dissociation of the proton into a system Y (Fig. 1d) represents a background to DPP, which contributes due to the limited detector acceptance in the forward (p-beam direction) region. This background is modelled by the DIFFVM generator [4] and is statistically subtracted from the data.

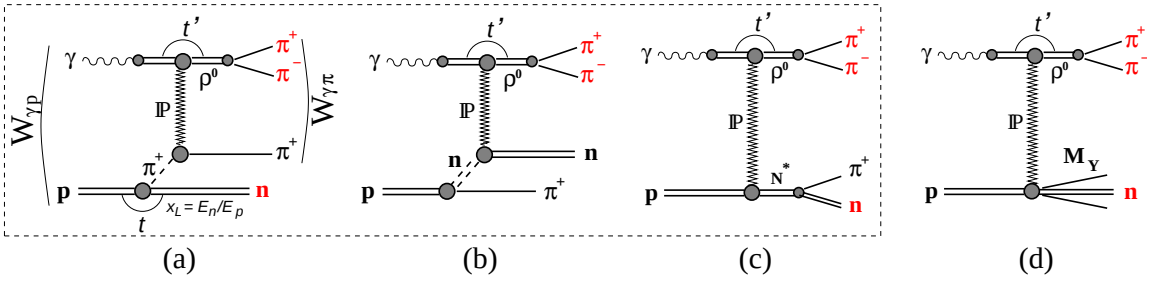

Figure 1: Generic diagrams for processes contributing to exclusive photoproduction of ρ^0 mesons associated with leading neutrons at HERA. The signal corresponds to the Drell-Hiida-Deck model graphs for the pion exchange (a), neutron exchange (b) and direct pole (c). Diffractive scattering in which a neutron may be produced as a part of the proton dissociation system, M_Y, contributes as background (d). The N^* in (c) denotes both resonant (via N^+) and possible non-resonant $n+\pi^+$ production.

2. Analysis Outline and Main Results

Using VDM [5] flux $f_{\gamma/e}(y,Q^2)$ to convert ep cross section into γp one, and one-pion-exchange approximation [6] to decompose photon-proton cross section into a pion flux convoluted with a photon-pion cross section one obtains for the reaction of interest $e+p \to e+\rho^0+n+\pi^+$

$$\frac{\mathrm{d}^2\sigma_{ep}}{\mathrm{d}y\mathrm{d}Q^2} = f_{\gamma/e}(y,Q^2)\sigma_{\gamma p}(W_{\gamma p}(y)); \qquad \frac{\mathrm{d}^2\sigma_{\gamma p}(W_{\gamma p},x_L,t)}{\mathrm{d}x_L\mathrm{d}t} = f_{\pi/p}(x_L,t)\,\sigma_{\gamma\pi}(W_{\gamma\pi}), \tag{2.1}$$

with the generic form of the pion flux factor [7]:

$$f_{\pi/p}(x_L,t) = \frac{1}{2\pi}\frac{g^2_{p\pi n}}{4\pi}(1-x_L)^{\alpha_{I\!P}(0)-2\alpha_\pi(t)}\frac{-t}{(m_\pi^2-t)^2}F^2(t,x_L). \tag{2.2}$$

Here $\alpha_{I\!P}(0)$ is the Pomeron intercept, $\alpha_\pi(t) = \alpha'_\pi(t - m_\pi^2)$ is the pion trajectory, $g^2_{p\pi n}/4\pi$ is the $p\pi n$ coupling constant known from phenomenological analysis of low energy data, and $F(t, x_L)$ is a form factor accounting for off mass-shell corrections and normalised to unity at the pion pole, $F(m_\pi^2, x_L) = 1$. For exact definition of kinematic variables in eq. (2.1-2.2) see [8].

The analysis is based on ~ 6600 events, containing only two charged pions from ρ^0 decay and a leading neutron with energy $E_n > 120$ GeV, and nothing else above noise level in the detector. The sample corresponds to an integrated luminosity of 1.16 pb^{-1}, collected by a special minimum bias track trigger in the years 2006-2007 at $\sqrt{s_{ep}} = 319$ GeV. Further details of the analysis can be found in [8].

The effective mass distribution for two charged pions with $p_t > 200$ MeV each and within the central detector range $20^o < \theta < 160^o$ is shown in Fig. 2a. The distribution is corrected for the mass dependent detector efficiency. The sample is very clean with only 1.5% background contamination in the analysis region. The p_T dependent distortion of the Breit-Wigner line shape is shown in Fig. 2b. In Fig. 2c the spin-density matrix element r_{00}^{04} as measured in this experiment is compared to the values obtained at HERA for different Q^2 ranges.

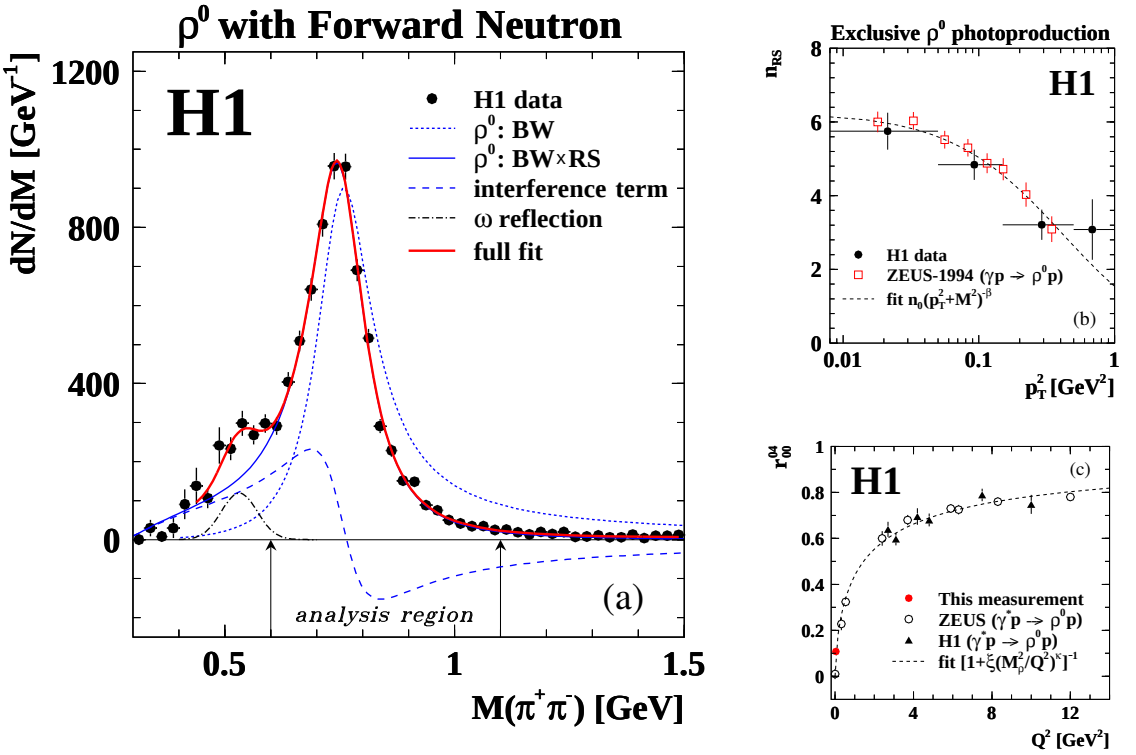

Figure 2: The ρ^0 meson properties: (a) Mass distribution of the $\pi^+\pi^-$ system with $p_T^2 < 1.0$ GeV^2. The data points are corrected for the detector efficiency. The curves represent different components contributing to the measured distribution and the Breit-Wigner resonant part extracted from the fit to the data. The analysis region $0.6 < M_{\pi^+\pi^-} < 1.1$ GeV is indicated by vertical arrows. (b) Ross-Stodolsky skewing parameter, n_{RS}, as a function of p_T^2 of the $\pi^+\pi^-$ system. The values measured in this analysis are compared to previously obtained results for elastic photoproduction of ρ^0 mesons, $\gamma p \to \rho^0 p$, by the ZEUS Collaboration. (c) Spin-density matrix element, r_{00}^{04}, as a function of Q^2 for diffractive ρ^0 photo- and electro-production. The curves on figures (b,c) represent the results of the fits discussed in [8].

After all selections described in [8] the remaining proton dissociative background fraction in the sample is estimated as 0.34 ± 0.05. This value is verified by normalising DIFFVM prediction to the orthogonal, background dominated sample, in which additional activity originating from M_Y system (see Fig.1d) in the forward region was required.

The γp cross section integrated in the domain $0.35 < x_L < 0.95$ and $p_{T,\rho} < 1$ GeV and averaged over the energy range $20 < W_{\gamma p} < 100$ GeV is determined for two intervals of leading neutron transverse momentum, corresponding to the full angular acceptance $\theta_n < 0.75$ mrad and the "OPE-safe" region respectively:

$$\sigma(\gamma p \to \rho^0 n\pi^+) = (310 \pm 6_{\text{stat}} \pm 45_{\text{sys}}) \text{ nb} \qquad \text{for} \qquad p_{T,n} < x_L \cdot 0.69 \text{ GeV} \tag{2.3}$$

$$\sigma(\gamma p \to \rho^0 n\pi^+) = (130 \pm 3_{\text{stat}} \pm 19_{\text{sys}}) \text{ nb} \qquad \text{for} \qquad p_{T,n} < 0.2 \text{ GeV}. \tag{2.4}$$

The differential cross section $\mathrm{d}\sigma_{\gamma p}/\mathrm{d}x_L$ is shown in Fig.3. Predictions from several π-flux models [7] are confronted with these data. Only a shape comparison is possible, since the $\gamma\pi$ cross section is not known. However, some models can be excluded even on the basis of this shape comparison.

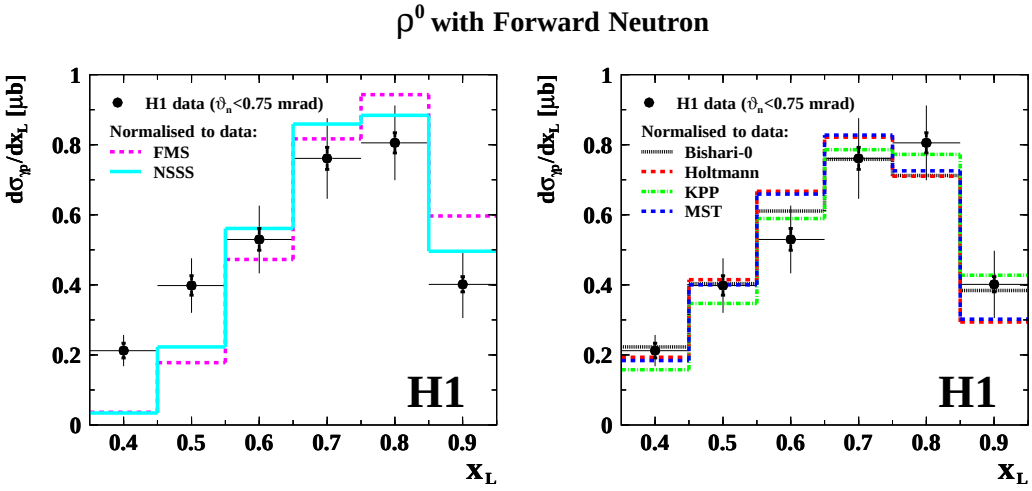

Figure 3: Differential cross section $\mathrm{d}\sigma_{\gamma p}/\mathrm{d}x_L$ in the range $20 < W_{\gamma p} < 100$ GeV compared to the predictions based on different versions of pion fluxes [7]. The data points are shown with statistical (inner error bars) and total (outer error bars) uncertainties, excluding an overall normalisation error of 4.4%. All predictions are normalised to the data.

Additional constraints on the pion flux models could be provided by the dependence on t (or $p^2_{T,n}$) of the leading neutron. The double differential cross section $\mathrm{d}^2\sigma_{\gamma p}/\mathrm{d}x_L\mathrm{d}p^2_{T,n}$ is measured, and the results are presented in Fig. 4 (left). The bins are chosen such, that the data are not affected by the polar angle cut. The cross sections are fitted by a single exponential function $e^{-b_n(x_L)p^2_{T,n}}$ in each x_L bin and the results are presented in Fig. 4 (right). The measured b-slopes are compared to those obtained from several pion flux parametrisations. Despite of the large experimental uncertainties none of the models is able to reproduce the data. This observation supports phenomenological expectation [9] of large absorptive corrections which modify the t dependence of the amplitude, leading to an increase of the effective b-slope at large x_L as compared to the pure OPE model without absorption.

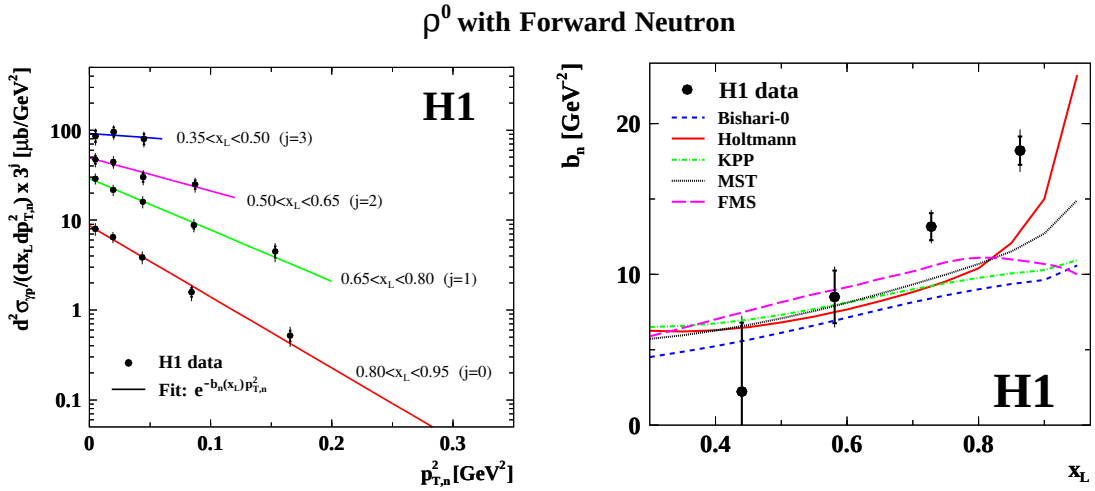

Figure 4: (left) Double differential cross section $\mathrm{d}^2\sigma_{\gamma p}/\mathrm{d}x_L\mathrm{d}p^2_{T,n}$ of neutrons in the range $20 < W_{\gamma p} < 100$ GeV fitted with single exponential functions. The cross sections in different x_L bins j are scaled by the factor 3^j for better visibility. The data points are shown with statistical (inner error bars) and total (outer error bars) uncertainties excluding an overall normalisation error of 4.4%. (right) The exponential slopes fitted through the p^2_T dependence of the leading neutrons as a function of x_L. The inner error bars represent statistical errors and the outer error bars are statistical and systematic errors added in quadrature. The data points are compared to the expectations of several parametrisations of the pion flux within the OPE model.

Fig. 5 (left) shows the energy dependence of exclusive ρ^0 production with a leading neutron, $\sigma_{\gamma p\to\rho^0 n\pi^+}(W_{\gamma p})$. Regge motivated fit $\sigma_{\gamma p} \propto W^{\delta}$ yields a value of $\delta = -0.26 \pm 0.06_{\mathrm{stat}} \pm 0.07_{\mathrm{sys}}$. POMPYT MC predicts different trend, typical for Pomeron exchange only.

The pion flux models compatible with the data in shape of the x_L distribution are used to extract the photon-pion cross sections from $\mathrm{d}\sigma/\mathrm{d}x_L$ in the OPE approximation. The result is presented in in Fig. 5 (right). As a central value the Holtmann flux is used, and the largest difference to the other three predictions (*Bishari-0, KPP, MST*) [7] provides an estimate of the model uncertainty which is $\sim$19% on average. From the total γp cross section in equation (2.4) and using the pion flux (2.2) integrated in x_L and $p_{T,n}$, $\Gamma_\pi = 0.056$, the cross section of elastic photoproduction of ρ^0 on a pion target is determined at an average energy $\langle W_{\gamma\pi}\rangle \simeq 24$ GeV:

$$\sigma(\gamma\pi^+ \to \rho^0\pi^+) = (2.33 \pm 0.34(\mathrm{exp})^{+0.47}_{-0.40}(\mathrm{model}))\ \mu\mathrm{b}, \tag{2.5}$$

where the model error is due to the uncertainty in the pion flux integral obtained for the different flux parametrisations compatible with our data. This value leads to the ratio $r_{\mathrm{el}} = \sigma^{\gamma\pi}_{\mathrm{el}}/\sigma^{\gamma p}_{\mathrm{el}} = 0.25 \pm 0.06$. A similar ratio, but for the total cross sections at $\langle W\rangle = 107$ GeV, has been estimated by the ZEUS collaboration as $r_{\mathrm{tot}} = \sigma^{\gamma\pi}_{\mathrm{tot}}/\sigma^{\gamma p}_{\mathrm{tot}} = 0.32 \pm 0.03$ [10]. Both ratios are significantly smaller than their respective expectations, based on simple considerations. For r_{tot}, a value of $2/3$ is predicted by the additive quark model, while $r_{\mathrm{el}} = (\frac{b_{\gamma p}}{b_{\gamma\pi}}) \cdot (\sigma^{\gamma\pi}_{\mathrm{tot}}/\sigma^{\gamma p}_{\mathrm{tot}})^2 = 0.57 \pm 0.03$ can be deduced by combining the optical theorem, the eikonal approach and the world data on pp, π^+p and γp elastic scattering. Such a suppression of the cross section is usually attributed to rescattering, or absorptive corrections [9], which are essential for leading neutron production. For the exclusive reaction $\gamma p \to \rho^0 n\pi^+$ studied here this would imply an absorption factor of $K_{abs} = 0.44 \pm 0.11$.

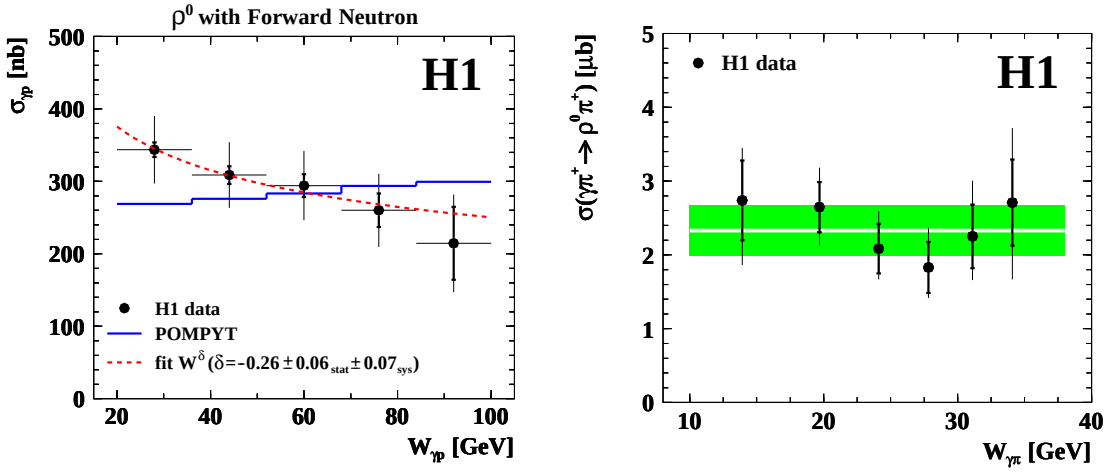

Figure 5: (left) Cross section of the reaction $\gamma p \to \rho^0 n\pi^+$ as a function of $W_{\gamma p}$ compared to the prediction from POMPYT MC program, which is normalised to the data. The dashed curve represents the Regge motivated fit $\sigma \propto W^\delta$ with $\delta = -0.26 \pm 0.06_{\rm stat} \pm 0.07_{\rm sys}$. The data points are shown with statistical (inner error bars) and total uncertainties (outer error bars) excluding an overall normalisation error of 4.4%. (right) Elastic cross section, $\sigma^{\rm el}_{\gamma\pi} \equiv \sigma(\gamma\pi^+ \to \rho^0\pi^+)$, extracted in the one-pion-exchange approximation as a function of the photon-pion energy, $W_{\gamma\pi}$. The inner error bars represent the total experimental uncertainty and the outer error bars are experimental and model uncertainties added in quadrature, where the model error is due to pion flux uncertainties. The dark shaded band represents the average value for the full $W_{\gamma\pi}$ range.

Finally, the cross section as a function of the four-momentum transfer squared of the ρ^0 meson, t', is presented in Fig. 6. It exhibits the very pronounced feature of a strongly changing slope between the low-t' and the high-t' regions, a feature known to be a characteristic for DPP reactions [1]. In a geometric picture, the large value of b_1 suggests that for a significant part of the data ρ^0 mesons are produced at large impact parameter values of order $\langle r^2 \rangle = 2b_1 \cdot (\hbar c)^2 \simeq 2\text{fm}^2 \approx (1.6R_{\rm p})^2$. In other words, photons find pions in a cloud which extends far beyond the proton radius. The small value of b_2 corresponds to a target size of $\sim$0.5 fm.

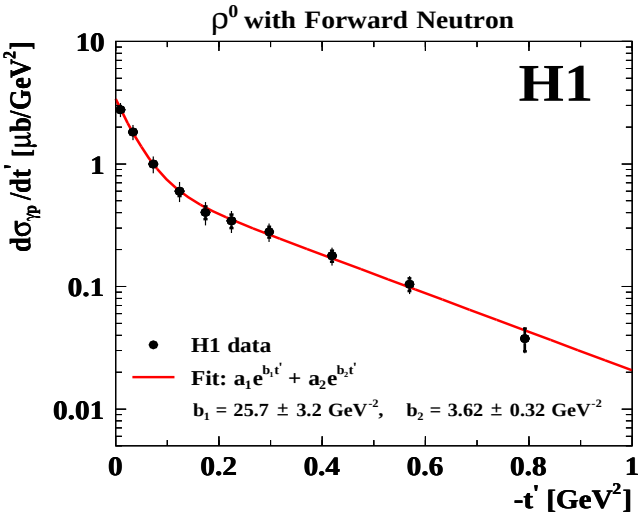

Figure 6: Differential cross section $\mathrm{d}\sigma_{\gamma p}/\mathrm{d}t'$ of ρ^0 mesons fitted with the sum of two exponential functions. The inner error bars represent statistical and uncorrelated systematic uncertainties added in quadrature and the outer error bars are total uncertainties, excluding an overall normalisation error of 4.4%. The values of slopes are characteristic for double peripheral processes [1] in which an exchange of two Regge trajectories is involved.

3. Summary

Photoproduction cross section for exclusive ρ^0 production associated with leading neutron is studied for the first time at HERA. Single and double differential γp cross sections are measured. The differential cross section $\mathrm{d}\sigma/\mathrm{d}t'$ shows the behaviour typical for exclusive double peripheral exchange processes. The elastic photon-pion cross section, $\sigma(\gamma\pi^+ \to \rho^0\pi^+)$, at $\langle W \rangle = 24$ GeV is extracted in the OPE approximation. The estimated cross section ratio for the elastic photoproduction of ρ^0 mesons on the pion and on the proton, $r_{\mathrm{el}} = \sigma_{\mathrm{el}}^{\gamma\pi}/\sigma_{\mathrm{el}}^{\gamma p} = 0.25 \pm 0.06$, suggests large absorption corrections, of the order of 60%, suppressing the rate of the studied reaction $\gamma p \to \rho^0 n\pi^+$.

References

[1] N.F. Bali, G.F. Chew and A. Pignotti, *Phys. Rev. Lett.* **19** (1967) 614;
G.F. Chew and A. Pignotti, *Multiperipheral Bootstrap Model*, *Phys. Rev.* **176** (1968) 2112;
E.L. Berger, *Phys. Rev.* **179** (1969) 1567.

[2] S.D. Drell and K. Hiida, *Phys. Rev. Lett.***7** (1961) 199; R.T. Deck, *Phys. Rev. Lett.***13** (1964) 169;
L.A. Ponomarev, Sov. J. Part. Nucl. **7** (1976) 70;
F. Hayot *et al.*, Lett. Nuovo Cim. **18** (1977) 185;
G. Cohen-Tannoudji, A. Santoro and M. Souza, *Nucl. Phys.* **B125** (1977) 445;
N.P. Zotov and V.A. Tsarev, Sov. J. Part. Nucl. **9** (1978) 266.

[3] P. Bruni and G. Ingelman, *Diffractive hard scattering at e p and p anti-p colliders*, in proceedings of the *Europhysics Conference*, C93-07-22, Marseille, France (1993) 595.

[4] B. List and A. Mastroberardino, *DIFFVM - A Monte Carlo generator for diffractive processes in ep scattering*, Proc. of the Workshop on Monte Carlo Generators for HERA Physics, eds. A.T. Doyle et al., DESY-PROC-1999-02 (1999) 396.

[5] J.J. Sakurai, Annals Phys. **11** (1960) 1;
J.J. Sakurai, *Phys. Rev. Lett.***22** (1969) 981;
T.H. Bauer *et al.*, Rev. Mod. Phys. **50** (1978) 261.

[6] J. D. Sullivan, *Phys. Rev.* **D5** (1972) 1732;
V. Pelosi, "One-pion exchange and inclusive reactions", Lett. Nuovo Cim. **4** (1972) 502;
G. Levman and K. Furutani, "Virtual pion scattering at HERA", DESY-95-142 (1995)

[7] (a) M. Bishari, *Pion exchange and inclusive spectra*, *Phys. Lett.* **B38** (1972) 510;
(b) H. Holtmann, A. Szczurek and J. Speth *Nucl. Phys.* **A596** (1996) 631; M.Przybycien, A.Szczurek and G.Ingelman, *Z. Phys.* **C74** (1997) 509;
(c) B.Kopeliovich, B.Povh and I.Potashnikova, *Z. Phys.* **C73** (1996) 125;
(d) W. Melnitchouk, J. Speth and A.W.Thomas, (e) L. Frankfurt, L. Mankiewicz and M. Strikman, *Z. Phys.* **A334** (1989) 343;
(f) N.N. Nikolaev, W.Schäfer, A. Szczurek and J. Speth, *Phys. Rev.* **D60** (1999) 014004.

[8] V. Andreev *et al.* [H1 Collaboration], *Eur. Phys. J.* **C76** (2016) 41.

[9] N. Nikolaev, J. Speth and B.G. Zakharov, hep-ph/9708290;
U. D'Alesio and H.J. Pirner, *Eur. Phys. J.* **A7** (2000) 109 [hep-ph/9806321];
A.B. Kaidalov *et al.*, *Eur. Phys. J.* **C47** (2006) 385 [hep-ph/0602215];
B.Z. Kopeliovich *et al.*, *Phys. Rev.* **D85** (2012) 114025 [arXiv:1205.0067].

[10] S. Chekanov *et al.* [ZEUS Collaboration], *Nucl. Phys.* **B637** (2002) 3.